Magnetic properties of graphene quantum dots

T. Espinosa-Ortega,[1,2] I. A. Luk'yanchuk,[3] and Y. G. Rubo[1]

[1]*Instituto de Energías Renovables, Universidad Nacional Autónoma de México, Temixco, Morelos 62580, México*
[2]*Division of Physics and Applied Physics, Nanyang Technological University, 637371 Singapore*
[3]*LPMC, University of Picardie Amiens, 80000 Amiens, France and Landau Institute for Theoretical Physics, 119334 Moscow, Russia*

Using the tight-binding approximation we calculated the diamagnetic susceptibility of graphene quantum dots (GQDs) of different geometrical shapes and characteristic sizes of 2–10 nm, when the magnetic properties are governed by the electron edge states. Two types of edge states can be discerned: the zero-energy states (ZESs), located exactly at the zero-energy Dirac point, and the dispersed edge states (DESs), with the energy close but not exactly equal to zero. DESs are responsible for a temperature-independent diamagnetic response, while ZESs provide a temperature-dependent spin paramagnetism. Hexagonal, circular, and randomly shaped GQDs contain mainly DESs, and, as a result, they are diamagnetic. The edge states of the triangular GQDs are of ZES type. These dots reveal the crossover between spin paramagnetism, dominating for small dots and at low temperatures, and orbital diamagnetism, dominating for large dots and at high temperatures.

PACS number(s): 73.22.Pr, 73.21.La, 75.20.−g, 75.75.−c

I. INTRODUCTION

In past years special attention has been paid to the fabrication of graphene quantum dots (GQDs),[1,2] susceptible to be used for magnetic-field-controlled spin-electronic logic gates.[3] The recently studied orbital[4–9] and spin[10–12] magnetism of such structures is actually a hot topic. However, the origin of the orbital diamagnetism, its relation with the edge-localized states, and its interplay with spin-paramagnetic effects require a more detailed study. This concerns, in particular, the dependence of the diamagnetic response on the size and shape of a GQD.

Landau diamagnetism in a perfect infinite graphene sheet was first studied by McClure[13,14] and Sharma *et al.*[15] and more recently in Refs. [16–20], where a singular behavior of susceptibility was found when the Fermi energy approaches the Dirac point at zero temperature. This peculiar behavior around zero energy also takes place in the cases in which a disorder-provided band is present for infinite graphene and ribbons.[21–25] On the other hand, the presence of the edge states with energy around zero is a signature of graphene nanoflakes with various terminations and most notably with zig-zag edges. Note that for nanoflakes with armchair termination the edge states are absent, since the two sublattices that form the honeycomb lattice are locally and globally balanced.[26–28]

The number and the properties of edge states are sensitive to the geometry of the GQD.[29–31] Since diamagnetism of graphene occurs due to the electronic states with energy near the Dirac point, it is natural to assume that the edge states should make a dominant contribution to magnetism of graphene nanoflakes, and the geometry of GQDs will play an important role in the diamagnetic response of the nanostructure.

In this paper we study the hexagonal, circular, triangular, and random GQDs with zigzag termination, and we identify two types of edge states. First, there are the dispersed edge states (DESs) whose energies are distributed in the range of 2Δ around the Dirac point, with the value of Δ being inversely proportional to the size of the GQD. Second, there could be highly degenerate exactly-zero-energy states (ZESs).

The DESs are appropriate to the hexagonal, circular, and random GQDs. Their energies are sensitive to an applied field that induces edge currents. These states provide the orbital diamagnetic response of the nanoflakes. The number of ZESs, which are mostly present in triangular GQDs, can be found exactly from graph theory.[32] Their origin is purely geometric, and their location does not change as a function of the applied magnetic field. Therefore, ZESs do not contribute to the diamagnetism of GQDs, but they can be occupied by electrons with unpaired spins and provide the paramagnetism of the system.[11] Studying the edge-state-provided orbital-diamagnetic and spin-paramagnetic response of GQDs we predict the possibility of crossover between paramagnetic and diamagnetic response of GQDs as a function of their shape, size, and temperature.

After this work was completed, we became aware of the work[33] in which similar research was done. The main difference between our results is that we consider dots of smaller size and at low temperatures $k_B T \ll \Delta$, where the edge-states-provided diamagnetic peak is broadened by size effects and is temperature independent. Reference 33 mainly addresses temperature effects relevant for GQDs with bigger sizes and small values of Δ when diamagnetism is mainly of the bulk origin.

II. THE MODEL OF GRAPHENE QUANTUM DOTS

We use the simplest nearest-neighbor tight-binding approximation. The properties of conducting π-electrons of graphene are described by the Hamiltonian

$$H = \sum_i \varepsilon_i c_i^\dagger c_i + \sum_{\langle ij \rangle} t_{ij} c_i^\dagger c_j, \tag{1}$$

where $c_i^\dagger$ and c_i are the creation and annihilation electron operators, respectively, and ε_i is the on-site energy. In what follows we do not consider any on-site disorder and set $\varepsilon_i = 0$. The hopping matrix elements t_{ij} between nearest-neighbor carbon atoms account for the magnetic field via the Peierls

substitution:

$$t_{ij} = \gamma_0 \exp\left\{\frac{e}{\hbar c}\int_{\mathbf{r}_i}^{\mathbf{r}_j}\mathbf{A}\cdot d\mathbf{l}\right\}, \qquad (2)$$

where $\mathbf{A} = (0, Bx, 0)$ is the vector potential of the magnetic field and the zero-field hopping was taken as $\gamma_0 = 3.0\,\mathrm{eV}$.

Graphene flakes were selected of hexagonal, circular, triangular, and random shapes with mostly zig-zag edges. The contour of the random shape nanostructures has been defined in polar coordinates by

$$r(\theta) = r_0 + \sum_{k=1}^{k_{\max}}[A_k\cos(k\theta) + B_k\sin(k\theta)], \qquad (3)$$

where r_0 is the constant average radius that defines the typical size of the flakes and A_k and B_k are random numbers with amplitude not exceeding $r_0/3$. In order to have realistic variation of the flake edge on the scale of the lattice constant, the maximum number of harmonics $k_{\max}$ has been chosen to be of the order of r_0/a, where $a = 2.461\,\mathring{\mathrm{A}}$ is the lattice constant. Typically, this number was about 25.

Direct numerical diagonalization of Hamiltonian Eq. (1) gives the field-dependent energy levels $E_n(B)$ and corresponding on-site amplitudes $\varphi_{n,i}$ of the wave function. The orbital energy of the π electrons at zero temperature as a function of the chemical potential μ and magnetic field B is given by

$$U(B,\mu) = 2\sum_{n}^{E_n<\mu} E_n(B), \qquad (4)$$

where the factor of 2 is the spin degeneracy of the levels. The low-temperature diamagnetic susceptibility per unit area has been calculated as

$$\chi(\mu) = -\frac{1}{\sigma}\left[\frac{\partial^2 U(B,\epsilon)}{\partial B^2}\right]_{B=0}, \qquad (5)$$

where $\sigma = \sqrt{3}a^2 N/4$ is the area of a graphene flake containing N carbon atoms.

III. BULK AND EDGE STATES

In what follows it will be convenient to distinguish between the bulk and the edge electronic states using the following geometrical criterion. For a given state with energy E_n we ascribe the intensity $I_n^{(b)} = \sum_{r_i<R}|\varphi_{n,i}|^2$ of the electronic states located within the circle of radius R to the *bulk* part of the total wave-function intensity, whereas the outer part $I_n^{(e)} = \sum_{r_i>R}|\varphi_{n,i}|^2 = 1 - I_n^{(b)}$ will be due to the *edge* contribution. The radius R has been chosen to be about one lattice constant smaller than the radius of the maximum circle that can be inscribed in a given GQD. Then, the state will be referred to as an edge state if $I_n^{(e)} > I_n^{(b)}$. Otherwise, we refer to it as a bulk state. Wave functions of the typical edge and bulk states are illustrated in Fig. 1.

The bulk and edge states distinguished by the above criterion are also separated in energy. Namely, the edge states normally possess the energy $|E| < \Delta$, while the energy of bulk states $|E| > \Delta$. We will refer to the energy interval of 2Δ around the Dirac point as the edge-states energy domain. It turns out that the value of the edge-states energy domain is
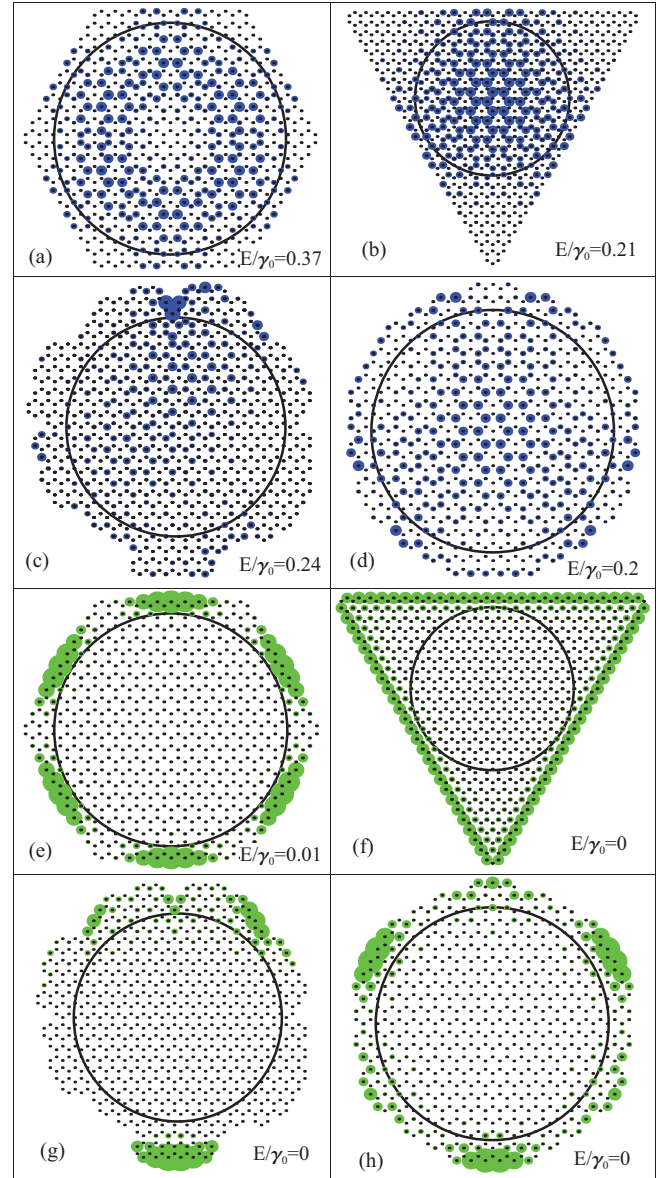
FIG. 1. (Color online) Amplitude of the wave function for bulk (a–d) and edge (e–h) states in GQDs of different shapes. We also show the maximal inscribed circles that have been used to discern between bulk and edge states.

approximately equal for all GQDs, characterized by the same inner radius R (see Fig. 2). The edge-states energy domain scales as $\Delta \propto \gamma_0/\sqrt{N} \propto \gamma_0 a/R$.

Two types of edge states can be discerned: (i) the zero-energy states (ZESs) that are degenerate and located exactly at $E = 0$, i.e., in the middle of the edge-states domain; and (ii) the dispersed edge states (DESs) that have nonzero energies, are symmetrically distributed with respect to $E = 0$, and fill the edge-states domain.

As has been shown by the graph theory[32] the total number of ZESs is related to the imbalance between the A- and B-type atoms in the graphene flake:

$$\eta_0 \geqslant |N_A - N_B|, \qquad (6)$$
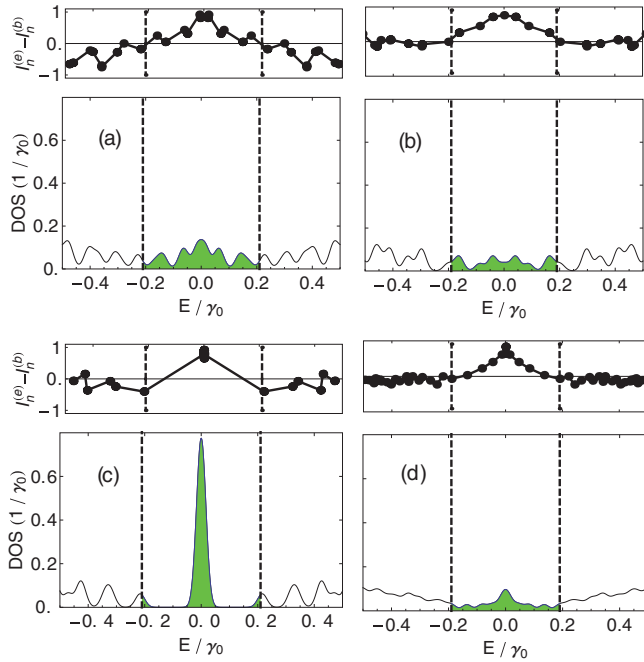
FIG. 2. (Color online) Electronic density of states and the difference of the edge and the bulk contributions intensities $I_n^{(e)} - I_n^{(b)}$ (see text) as a function of energy for the hexagonal (a), circular (b), triangular (c), and random (d) GQDs. The shaded region indicates the edge-states domain where the edge states are located. The levels have been artificially shown as Gaussian peaks with the dispersion 0.05 eV.

where equality takes place for the geometry of equilateral polygons. For hexagons $\eta_0 = 0$, there are no ZESs and all edge states are of the DES type. In contrast, for the equilateral triangles all the edge states are of ZES type and their degeneracy number is given by[6,7]

$$\eta_0^\Delta = \sqrt{N + 3} - 3. \tag{7}$$

Usually, there are only a few ZESs for circular and randomly shaped GQDs.

The number and positions of ZESs do not depend on magnetic field, and therefore these levels do not contribute to the orbital part of the susceptibility Eq. (5) within the simple tight-binding approximation Eq. (1). (Note, however, that the degeneracy of ZESs is lifted when one accounts for the next-nearest-neighbor hopping in the tight-binding Hamiltonian; in this case, applied magnetic field would also affect the position of these levels, and some ZES-related contribution to diamagnetism can appear.) In contrast, they are responsible for the spin-provided superparamagnetic response of an ensemble of clusters in the case of a half-filled π band when the Fermi energy is pinned at $\mu = 0$. Indeed, according to the Hund theorem, the number of single occupied states of a degenerate level should be maximal, providing the total uncompensated spin defined by Lieb's rule[11,12] $S = \frac{1}{2}\eta_0$, which brings a substantial contribution to the temperature-dependent spin-Curie paramagnetism.

On the other hand, the location of DESs in hexagonal, circular, and random GQDs depends on the applied field,

and therefore these levels are responsible for diamagnetism of graphene clusters, as calculated below.

IV. HEXAGONS, CIRCLES, AND RANDOM QUANTUM DOTS

The susceptibility was calculated for zig-zag edge hexagons and circles of about ten different sizes, having an inner radius in the range of 2–7 nm. For random quantum dots, the averaging has been performed over three different ensembles, characterized by mean inner radii $R_1 = 2.6$ nm, $R_2 = 3.65$ nm, and $R_3 = 4.69$ nm, with the standard deviation for each ensemble being $\sigma_1 = 39.1$, $\sigma_2 = 75.1$, and $\sigma_3 = 152.2$, respectively. The magnetic field varied between 0 and 5 T, a range in which the
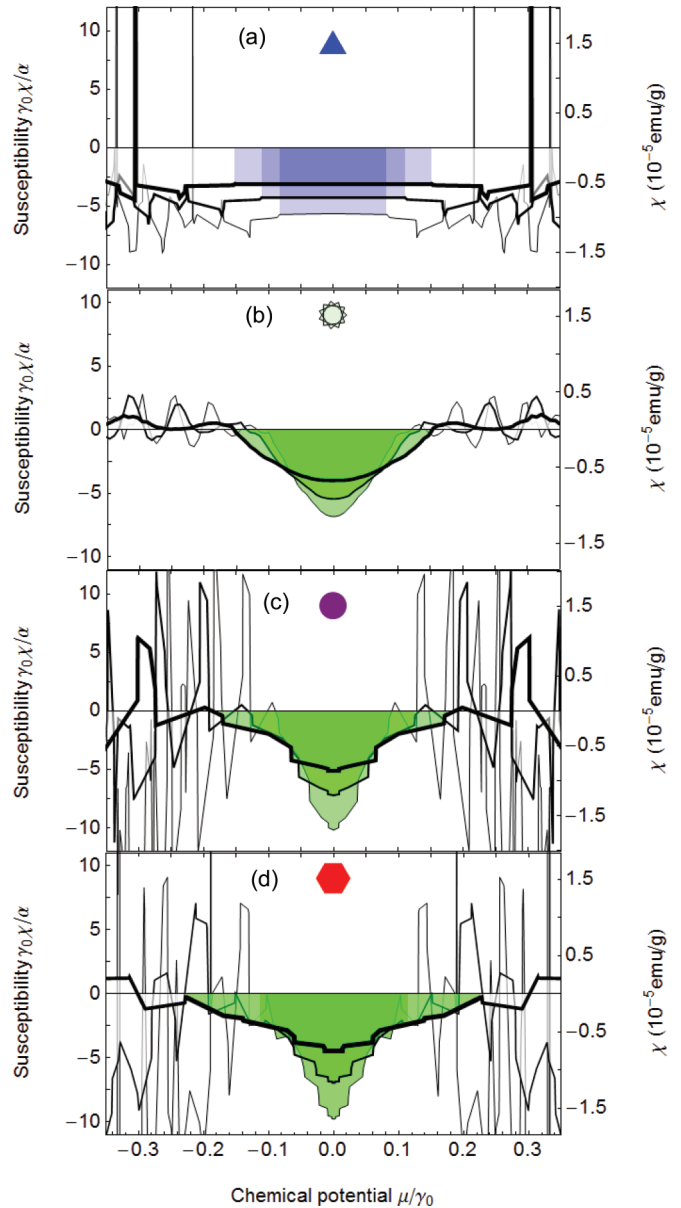
FIG. 3. (Color online) Susceptibility for triangular (a), random (b), circular (c), and hexagonal (d) GQDs; we show three different sizes ranging from 2–7 nm. The shaded region indicates the edge-states domain, and the thickness of the line increases as the size of the GQD decreases.

susceptibility remained approximately constant. All the plots are presented for $B = 5$ T. Figure 2 shows the density of states as a function of the Fermi energy for hexagonal and random shape GQDs. The shaded area indicates the region where the edge states are located.

Figure 3 shows the magnetic susceptibility per unit of area as a function of the Fermi energy for GQDs of different sizes. As was qualitatively explained above, the diamagnetic peak of width 2Δ appears when the chemical potential crosses the edge-states domain. This peak becomes wider with decreasing of the GQD size. Beyond this zone, the orbital susceptibility is a highly fluctuating function of the Fermi energy that oscillates between paramagnetic and diamagnetic signs. These oscillations have been recently interpreted for graphene ribbons, as a result of the sub-band structure.[25]

As mentioned above, the number of ZESs for these geometries is vanishingly small and the spin Curie-type paramagnetism is absent. Note, however, that electron-electron correlation can provide the site-alternating ordering of localized spins along the GQD edges,[11] giving the paramagnetic contribution. Such an effect, which can be discerned experimentally by electron-spin-resonance measurements, is beyond the scope of our article.

V. TRIANGULAR QUANTUM DOTS

All the edge states in triangular GQDs with zig-zag edges are of ZES type, which does not change its energy as a function of the field and does not contribute to the diamagnetic susceptibility. The ZESs for GQDs of different sizes are located in the middle of the gap 2Δ, as shown in Fig. 4. We note that 2Δ indicates the real gap in the spectrum for the triangular GQDs, and the value of this gap is inversely proportional to the number of ZESs η_0^Δ:

$$\Delta = \frac{\zeta \gamma_0}{\eta_0^\Delta} = \frac{\zeta \gamma_0}{\sqrt{(N+3)} - 3}, \tag{8}$$

where the numerical constant is $\zeta \simeq 5.56$.

The magnetic susceptibility of triangular GQDs χ_{orb}^Δ is shown in Fig. 3 for nine inner sizes of 2.5–7 nm. It is provided by the out-of-gap delocalized electronic states and does not depend on μ within the gap 2Δ because of the absence of DESs. These results match the analytical calculations of
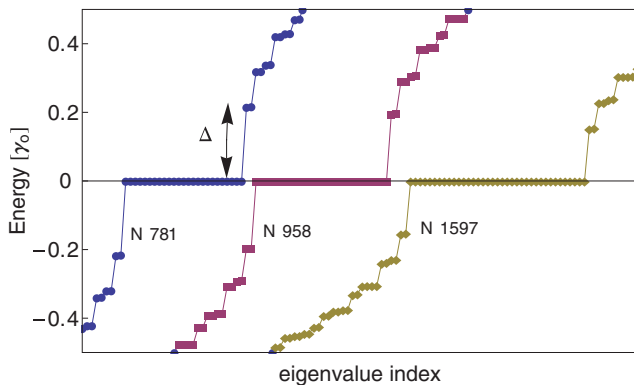
FIG. 4. (Color online) The band gap for triangular GQDs with different numbers of atoms N.

Refs. 20 and 24 for an infinite graphene sheet with the band gap 2Δ, according to which the diamagnetic susceptibility per unit area is

$$\chi_{\text{orb}}^\Delta(\mu) = -\alpha \frac{\theta(\Delta - |\mu|)}{2\Delta}, \qquad \alpha = \frac{e^2 \gamma_0^2 a^2}{2\pi \hbar^2 c^2}, \tag{9}$$

where $\theta(x)$ is the step function.

Although ZESs give no contribution to the orbital susceptibility, they can be responsible for the huge paramagnetism provided by η_0 uncompensated electron spins located on the degenerate ZES levels. This happens in the case of small positive chemical potentials if the energy of electron-electron repulsion in each zero-energy state $U_{e-e} > \mu$, so that these levels remain half filled. The corresponding Curie-type temperature-dependent paramagnetic susceptibility for noninteracting electrons is evaluated per unit area as

$$\chi_{\text{spin}}^\Delta = \frac{\eta_0^\Delta}{\sigma} \frac{(g\mu_B)^2}{3} \frac{s(s+1)}{k_B T} = \frac{\eta_0^\Delta \mu_B^2}{\sigma k_B T}, \tag{10}$$

where μ_B is the Bohr magneton and $g \simeq 2$ is the g factor of the electrons with spin $s = 1/2$.

In the opposite case of the strong Coulomb electron correlations, according to the Lieb theorem,[34] all $\eta_0^\Delta \gg 1$ ZES electrons form the total spin of the cluster $S = \eta_0/2$. The superparamagnetic susceptibility of an ensemble of triangular GQDs becomes even stronger:

$$\chi_{\text{spin}}'^\Delta = \frac{1}{\sigma} \frac{(g\mu_B)^2}{3} \frac{S(S+1)}{k_B T} \simeq \frac{(\eta_0^\Delta \mu_B)^2}{3\sigma k_B T}. \tag{11}$$

It should be noted that in the limit of strong electron-electron correlations the electron-hole symmetry might be broken. This would affect the total magnetism of the system, especially when the chemical potential is moved away from the Fermi energy.[35] The actual value of paramagnetic susceptibility must be somewhere between $\chi_{\text{spin}}^\Delta$ and $\chi_{\text{spin}}'^\Delta$.

Using Eqs. (15) and (11) we compare the spin-paramagnetic and orbital-diamagnetic contributions at $\mu = 0$, presenting their ratio for the case of strongly correlated electrons as

$$\left| \frac{\chi_{\text{spin}}'^\Delta}{\chi_{\text{orb}}^\Delta} \right| \simeq \frac{7.1 \text{ eV}}{\sqrt{N} k_B T}. \tag{12}$$

It follows that varying the size and temperature of the triangular quantum dots we can expect the paramagnetic-diamagnetic crossover. In particular, for a temperature of $T = 77$ K, we predict that triangular quantum dots will be paramagnetic for the inner radius below $R \simeq 97$ nm.

VI. SIZE DEPENDENCE

We calculated the diamagnetic susceptibilities, given by the gap-zone-integral, $\int_{-\Delta}^{\Delta} \chi(\mu) d\mu$ (the shaded area in Fig. 3). We found that, as the size of a GQD increases, the area is conserved and 2Δ vanishes. In the limit of an infinite cluster with $\Delta \to 0$ this gives the McClure δ peak of graphene orbital susceptibility:[13]

$$\chi(\mu) = -\alpha \delta(\mu). \tag{13}$$

The gap Δ vanishes as the number of atoms increases.[36] Here, we found that the dependence of Δ is similar for all shapes (see Fig. 5) and follows Eq. (8).
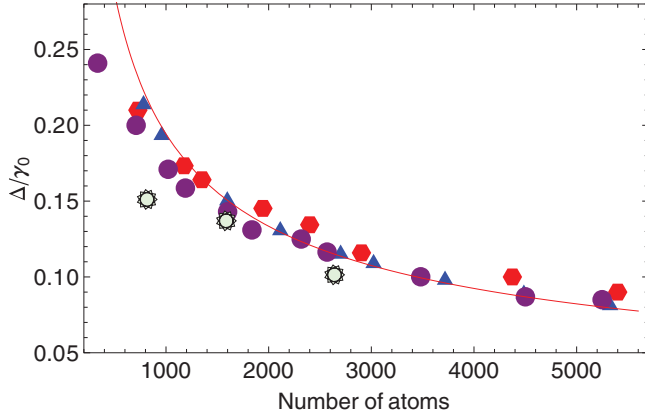
FIG. 5. (Color online) Δ dependence on the number of atoms in GQDs of different geometry.

The size dependence of the orbital susceptibility for hexagonal, circular, and random GQDs at $\mu = 0$ is shown in Fig. 6. It satisfies an empirical relation:

$$\chi_{\mathrm{orb}} = \beta N^{\lambda}, \tag{14}$$

with $\lambda = 0.4$ and $\beta = 0.31\alpha/\gamma_0$. Although the orbital diamagnetism originates from the edge currents of the low-energy DES, their perimeter contribution $\sim N^{1/2}$ can be reduced by the armchair- and/or zigzag-type boundary irregularities as well as by the wave function vanishing at the corners of GQDs, which explains the reduction of the exponent index λ slightly below $1/2$.

For triangular GQDs the size dependence of the orbital susceptibility can be obtained by substituting the value of Δ from Eq. (8) into Eq. (9) at $\mu = 0$:

$$\chi_{\mathrm{orb}}^{\Delta} = -\frac{\alpha}{\gamma_0} \frac{\sqrt{N+3}-3}{2\zeta}. \tag{15}$$

This estimation agrees with our numerical calculations, as shown in Fig. 6.

So far, there are no experimental measurements of magnetism of GQDs, but the susceptibility we obtained is in the range of the measured values for carbon nanotubes and buckyballs.[37] For convenience, we also presented the susceptibilities in units of emu/g, in Figs. 3 and 6.

VII. CONCLUSIONS

Magnetism of GQDs is provided by the edge states whose energy is located within the finite-size energy interval around the Dirac point: the edge-states energy domain. The structure of the edge-state spectrum and magnetic response of GQDs is strongly dependent on the geometric shape of the cluster.
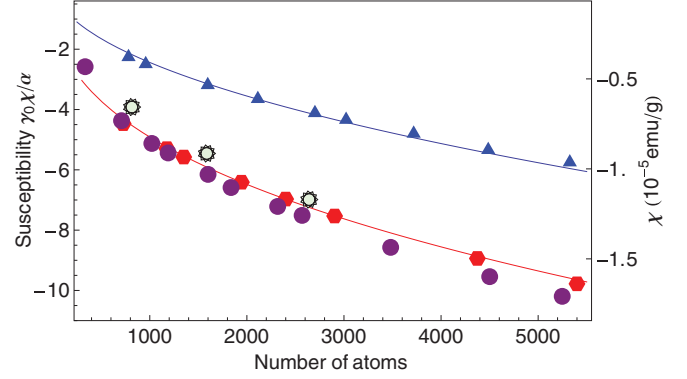
FIG. 6. (Color online) Dirac-point orbital susceptibility at $\mu = 0$. The solid lines correspond to the fit according to Eqs. (15) and (14).

For hexagonal, circular, and random GQDs the edge states are dispersed within the edge-states energy domain. Their position depends on the applied field, providing substantial diamagnetic response of GQDs. The diamagnetic susceptibility as a function of the chemical potential presents a peak of constant intensity, centered around $\mu = 0$. The maximum of the peak increases with the GQD size, whereas its width decreases, approaching the δ function of McClure[13] for an infinite sheet of graphene.

For triangular GQDs the edge states are located exactly at the middle of the gap with high degeneracy factor η_0^{Δ} given by Eq. (8) that increases with the size of the cluster. The zero-energy positions of these levels do not change with the field, and the diamagnetic response of triangular GQDs $\chi_{\mathrm{orb}}^{\Delta}$ is expected to be small. In contrast, the uncompensated spins of electrons localized at ZESs can provide a huge paramagnetic temperature-dependent contribution $\chi_{\mathrm{spin}}^{\Delta}$ of the Curie type. By comparison of susceptibilities $\chi_{\mathrm{orb}}^{\Delta}$ and $\chi_{\mathrm{spin}}^{\Delta}$, Eq. (12), we expect to have the crossover from paramagnetic to diamagnetic response in an ensemble of triangular clusters with increasing temperature and/or GQD size.

The strong dependence of magnetic properties of GQDs on their geometry, size, and temperature provides a natural way to separate graphene clusters according to their shape and size by application of an appropriately designed nonuniform magnetic field and temperature cycle that can trap different GQDs in different points of space. It would be interesting also to study specially cut nanoclusters of highly ordered pyrolytic graphite, which can contain separate graphene sheets with a Dirac-like spectrum[38] and therefore can have a similar magnetic behavior.

[1]J. Scott-Bunch *et al.*, Nano Lett. **5**, 287 (2005).

[2]B. Ozyilmaz, P. Jarillo-Herrero, D. Efetov, D. A. Abanin, L. S. Levitov, and P. Kim, Phys. Rev. Lett. **99**, 166804 (2007).

[3]W. L. Wang, O. V. Yazyev, S. Meng, and E. Kaxiras, Phys. Rev. Lett. **102**, 157201 (2009).

[4]Z. Z. Zhang, K. Chang, and F. M. Peeters, Phys. Rev. B **77**, 235411 (2008).

[5]S. Schnez, K. Ensslin, M. Sigrist, and T. Ihn, Phys. Rev. B **78**, 195427 (2008).

[6]P. Potasz, A. D. Güçlü, and P. Hawrylak, Phys. Rev. B **81**, 033403 (2010).

[7]M. Zarenia, A. Chaves, G. A. Farias, and F. M. Peeters, Phys. Rev. B **84**, 245403 (2011).

[8]M. Grujic, M. Zarenia, A. Chaves, M. Tadic, G. A. Farias, and F. M. Peeters, Phys. Rev. B **84**, 205441 (2011).

[9]I. A. Luk'yanchuk and A. M. Bratkovsky, Phys. Rev. Lett. **100**, 176404 (2008).

[10]M. Ezawa, Phys. Rev. B **76**, 245415 (2007).

[11]J. Fernandez-Rossier and J. J. Palacios, Phys. Rev. Lett. **99**, 177204 (2007).

[12]W. L. Wang, S. Meng, and E. Kaxiras, Nano Lett. **8**, 241 (2008).

[13]J. W. McClure, Phys Rev. **104**, 666 (1956).

[14]J. W. McClure, Phys Rev. **119**, 606 (1960).

[15]M. P. Sharma, L. G. Johnson, and J. W. McClure, Phys. Rev. B **9**, 2467 (1974).

[16]H. Fukuyama, J. Phys. Soc. Jpn. **76**, 043711 (2007).

[17]M. Nakamura, Phys Rev B **76**, 113301 (2007).

[18]A. Ghosal, P. Goswami, and S. Chakravarty, Phys. Rev. B **75**, 115123 (2007).

[19]S. Slizovskiy and J. J. Betouras, Phys. Rev. B **86**, 125440 (2012).

[20]S. G. Sharapov, V. P. Gusynin, and H. Beck, Phys. Rev. B **69**, 075104 (2004).

[21]K. Wakabayashi, M. Fujita, H. Ajiki, and M. Sigrist, Phys. Rev. B **59**, 8271 (1999).

[22]M. Koshino and T. Ando, Phys. Rev. B **75**, 235333 (2007).

[23]J. Liu, Z. Ma, A. R. Wright, and C. Zhang, J. Appl. Phys. **103**, 103711 (2008).

[24]M. Koshino and T. Ando, Phys. Rev. B **81**, 195431 (2010).

[25]Y. Ominato and M. Koshino, Phys. Rev. B **85**, 165454 (2012).

[26]K. Nakada, M. Fujita, G. Dresselhaus, and M. S. Dresselhaus, Phys. Rev. B **54**, 17954 (1996).

[27]M. Fujita, K. Wakabayashi, K. Nakada, and K. Kusakabe, J. Phys. Soc. Jpn. **65**, 1920 (1996).

[28]J. Wurm, K. Richter, and I. Adagideli, Phys. Rev. B **84**, 075468 (2011).

[29]H. P. Heiskanen, M. Manninen, and J. Akola, New J. Phys. **10**, 103015 (2008).

[30]T. Espinosa-Ortega, I. A. Luk'yanchuk, and Y. G. Rubo, Superlattices Microstruct. **49**, 283 (2011).

[31]A. V. Rozhkov, G. Giavaras, Y. P. Bliokh, V. Freilikher, and F. Nori, Phys. Rep. **503**, 77 (2011).

[32]S. Fajtlowicz, P. E. John, and H. Sachs, Croatica Chemica Acta **78**, 195 (2005).

[33]Y. Ominato and M. Koshino, Phys. Rev. B **87**, 115433 (2013).

[34]E. H. Lieb, Phys. Rev. Lett. **62**, 1201 (1989).

[35]A. D. Güçlü, P. Potasz, O. Voznyy, M. Korkusinski, and P. Hawrylak, Phys. Rev. Lett. **103**, 246805 (2009).

[36]A. D. Güçlü, P. Potasz, and P. Hawrylak, Phys. Rev. B **82**, 155445 (2010).

[37]S. Bandow, J. Appl. Phys. **80**, 1020 (1996).

[38]I. Luk'yanchuk, Y. Kopelevich, and M. El Marssi, Physica B: Cond. Matt. **404**, 404 (2009).